NASA Contractor Report 3330

A Rapid Implicit-Explicit Solution to the Two-Dimensional Time-Dependent Incompressible Navier-Stokes Equations

Joseph E. Davis

CONTRACT A50807B
OCTOBER 1980

NASA

NASA Contractor Report 3330

A Rapid Implicit-Explicit Solution to the Two-Dimensional Time-Dependent Incompressible Navier-Stokes Equations

Joseph E. Davis
Joseph E. Davis
Saratoga, California

Prepared for
Ames Research Center
under Contract A50807B

National Aeronautics
and Space Administration

Scientific and Technical
Information Branch

1980

A

A RAPID IMPLICIT-EXPLICIT SOLUTION TO THE TWO-DIMENSIONAL TIME-DEPENDENT INCOMPRESSIBLE NAVIER-STOKES EQUATIONS*

Joseph E. Davis
20780 Sevilla Lane, Saratoga, California

ABSTRACT

A rapid implicit-explicit finite difference scheme has been developed for the numerical solution of the time-dependent, incompressible, two-dimensional Navier-Stokes equations in conservation-law form using vorticity and stream function variables. The algorithm is second-order time-accurate and spatially factored. The systems of equations are solved at each time step by an iterative technique. Numerical results have been obtained with the technique for a circular cylinder at a Reynolds number of 15, and an NACA 0012 airfoil at zero angle of attack at Reynolds numbers of 10^3 and 10^4. The results are in agreement with another numerical technique, and the computing time required to obtain the steady-state solution at the Reynolds number of 10^4 was 49.7 sec on a CDC 7600 computer using a 65 × 84 computational grid.

INTRODUCTION

Rapid numerical solutions to the time-dependent Navier-Stokes equations at moderate Reynolds numbers and low Mach numbers have been difficult to obtain because of the elliptic nature of the equations in this regime. Unlike high Mach number compressible flows, each portion of the flow field significantly influences every other portion of the flow field which drastically increases the amount of computation time required to obtain either a time-accurate or steady-state numerical solution.

Fast numerical techniques developed for the solution of the compressible Navier-Stokes equations, such as the algorithms of MacCormack[1] and Beam and Warming,[2] unfortunately do not perform as efficiently in the low Mach number regime as they do at high Mach numbers. J. L. Steger (private communication) has applied the latter technique to the laminar flow (Re = 10^4) about an NACA 0012 airfoil at zero angle of attack and a Mach number of 0.2 and was able to obtain a steady-state solution on a 71 × 33 grid in about 20 min of computing time on a CDC 7600 computer.

Roache[3] has presented a fast numerical technique for the incompressible steady Navier-Stokes equations as applied to the internal flow in flush

---

*Work performed under Contract No. A50807B for Ames Research Center.

inlets. However, his program at present does not simulate unsteady flows and has only been tested on a very coarse mesh, where the number of iterations required to converge to a steady-state solution may be lower than the number required for a fine mesh. Other excellent numerical techniques for solving the incompressible time-dependent Navier-Stokes equations, such as the methods of Mehta,[10] Reddy and Thompson,[4] Wu,[5] and Thames,[6] all require approximately one-half hour or more of computing time on a CDC 7600 to obtain steady-state solutions for moderate Reynolds numbers ($\sim 10^4$) and sufficiently fine grids (~5000 mesh points). Even the very efficient method of Ghia, Hankey, and Hodge,[7] which was developed for cavity flows, appears to require about 4 min of computing time at these Reynolds numbers and grid sizes to obtain steady-state solutions. It is therefore the purpose of this report to present a rapid numerical technique for solving the incompressible time-dependent Navier-Stokes equations for the flow about two-dimensional airfoils using very fine computational grids.

The present numerical technique evolved as the result of an investigation intended to obtain numerical solutions to the incompressible time-dependent Navier-Stokes equations by utilizing the Newton-Kantorovich technique.[9] This technique is a rigorous mathematical concept based on functional analysis that transforms a nonlinear partial differential equation into a sequence of linear partial differential equations. When this technique is applied to a second-order time-accurate differencing of the Navier-Stokes equations and maximum advantage is taken of previous time step information, it reduces to approximating the Navier-Stokes equations by a single linear partial differential equation. The equation becomes linear because the nonlinear term has, in effect, been replaced by a first-order Taylor series expansion in function space. A detailed discussion of the mathematical foundations of the technique as well as a summary of previous investigations utilizing the technique are given in Gabrielsen[8] and Davis, Gabrielsen, and Mehta.[9]

As a result of that investigation, new insight was gained to improve the numerical technique used to solve the Navier-Stokes equations. This report describes these improvements and the results obtained to date using the improved technique.

MATHEMATICAL FORMULATION

The present numerical technique has been incorporated into a computer code that is restricted to symmetric flow fields and geometries. It is a special version of a more general computer code that was developed for nonsymmetric airfoils at angle of attack and is described in detail in reference 10. The mathematical formulation contained herein describes only the symmetric case, although the development for the angle of attack case is very similar.

The flow field and geometry under consideration are mapped into the unit half-circle. As a result of this transformation, the equation governing the

unsteady, incompressible flow of a Newtonian fluid may be expressed in terms of a transformed vorticity transport equation and disturbance stream function equation as

$$H^2 r^2 \frac{R}{L} \frac{\partial \omega}{\partial t} = \left(\frac{d\rho}{dr}\right)^2 r^2 \frac{\partial^2 \omega}{\partial \rho^2} + \left(\frac{d\rho}{dr} r + \frac{d^2\rho}{dr^2} r^2\right) \frac{\partial \omega}{\partial \rho} + \frac{\partial^2 \omega}{\partial \theta^2} - r \frac{d\rho}{dr} \frac{R}{L} J\left(\frac{\omega, \Psi}{\rho, \theta}\right) \quad (1)$$

and

$$r^2\left(\frac{d\rho}{dr}\right)^2 \frac{\partial^2 \psi}{\partial \rho^2} + \left(\frac{d\rho}{dr} r + \frac{d^2\rho}{dr^2} r^2\right) \frac{\partial \psi}{\partial \rho} + \frac{\partial^2 \psi}{\partial \theta^2} = -H^2 r^2 \omega \quad (2)$$

where

$$H^2 = \left(\frac{\partial x}{\partial r} \frac{\partial y}{\partial \theta} - \frac{\partial x}{\partial \theta} \frac{\partial y}{\partial r}\right) \Big/ r \quad (3)$$

and

ω = vorticity

Ψ = total stream function

ψ = disturbance stream function $\Psi - y$

(x,y) = coordinates of physical flow field

(r,θ) = coordinates of the interior of the unit half-circle where $0 \leq r \leq 1$ and $\pi \leq \theta \leq 2\pi$

ρ = stretched radial coordinate where the stretching function is defined below

L = dimensionless chord

R = Reynolds number Ul/ν

U = freestream velocity

l = chord

ν = kinematic viscosity

t = time

The term $J\left(\frac{\omega, \Psi}{\rho, \theta}\right)$ is the conservation-law form of the convective terms. That is,

$$J\left(\frac{\omega, \Psi}{\rho, \theta}\right) = \frac{1}{3}\left[\frac{\partial}{\partial \rho}\left(\frac{\partial \Psi}{\partial \theta} \omega\right) + \frac{\partial \Psi}{\partial \theta} \frac{\partial \omega}{\partial \rho} + \frac{\partial}{\partial \theta}\left(\Psi \frac{\partial \omega}{\partial \rho}\right) - \frac{\partial}{\partial \theta}\left(\omega \frac{\partial \Psi}{\partial \rho}\right) - \frac{\partial \Psi}{\partial \rho} \frac{\partial \omega}{\partial \theta} - \frac{\partial}{\partial \rho}\left(\Psi \frac{\partial \omega}{\partial \theta}\right)\right] \quad (4)$$

The radial coordinate r is transformed according to a function that stretches the region near the body surface ($r = 1$) so that proper resolution of the boundary layer and separation zone may be obtained. The stretched radial coordinate is depicted by the variable ρ and is expressed as

$$\rho = (k_1 + k_2)^{-1}[\tanh^{-1}(rk_3 - k_4) + k_2] \tag{5}$$

with

$$k_3 = \left[\tanh(k_1) + \tanh(k_2)\right]\left[1 - \frac{r_o}{(r_o - 1)}\right]$$

and

$$k_4 = \tanh(k_2) - r_o[\tanh(k_1) + \tanh(k_2)]\,\frac{1}{(r_o - 1)}$$

The constants r_o, k_1, and k_2 (all positive) determine the value of ρ. As r varies from r_o to 1, ρ varies from 0 to 1.

The mapping into the unit circle is accomplished by the transformation

$$z = \frac{1}{K} + \gamma + \frac{Kc^2}{1 + \gamma K} \tag{6}$$

where

$z = x + iy$

$K = re^{i\theta}$

$\gamma = \xi + i\eta$

A proper choice of the constants γ and c invokes the solution for the flow over any one of a number of shapes, including a flat plate, a circular or elliptical cylinder, or thick airfoils. The trailing edge of an airfoil shape may be rounded off by defining

$$c = \left[\xi + (1 - \eta^2)^{1/2}\right](1 - \delta)\ , \qquad \text{where} \quad 0 < \delta < 1 \tag{7}$$

The components of velocity u_1 and u_2 are defined in terms of the disturbance stream function as

$$u_1 = \frac{1}{rH}\left(\frac{\partial\psi}{\partial\theta} + \frac{\partial y}{\partial\theta}\right)\ , \qquad u_2 = -\frac{1}{H}\left(\frac{d\rho}{dr}\,\frac{\partial\psi}{\partial\rho} + \frac{\partial y}{\partial r}\right) \tag{8}$$

For Reynolds numbers much larger than unity, the vorticity in the flow field exists only near the body and in the wake. Away from this region, the flow is essentially irrotational; therefore, the region of calculation is

subdivided into two parts: a small viscous region and a large irrotational region bounded by ρ_o and ρ_r with $\pi \le \theta \le \theta_2$ (see fig. 1).

The boundary conditions applied along the boundaries of the region of calculation are shown in figure 1 as follows:

1. On the surface ($\rho = 1$), the constraint of no slip is applied in the form

$$\Psi = 0 \qquad (\text{or} \quad \psi = -y) \tag{9}$$

and

$$\frac{\partial \Psi}{\partial \rho} = 0 \tag{10}$$

Condition (10) is used to calculate the surface vorticity by the method of Israeli[11] described in detail later.

2. Along the line of symmetry, the vorticity ω and the disturbance stream function ψ are specified to be zero.

3. The flow at the far boundary is constrained with first-order differential relations obtained from the Navier-Stokes equations by dropping the tangential derivative of the pressure and viscous terms (i.e., at the outer boundary); the inertia terms are dominant:

$$H^2 r \frac{\partial \omega}{\partial t} = -\frac{d\rho}{dr} J\left(\frac{\omega, \Psi}{\rho, \theta}\right) \tag{11}$$

$$\frac{\partial \psi}{\partial \rho} = -\frac{dr}{d\rho}\left(u_2 H + \frac{\partial y}{\partial r}\right) \tag{12}$$

and u_2 is obtained from the θ component of the Navier-Stokes equation. That is,

$$\frac{\partial u_2}{\partial t} = -\left[\frac{1}{2rH} \frac{\partial (u_1^2 + u_2^2)}{\partial \theta} + u_1 \omega\right] \tag{13}$$

Note that, in equation (13), $\omega = 0$ when $\pi \le \theta \le \theta_2$. At $t = 0$, the flow is irrotational (without circulation), that is, $\omega = 0$ and $\psi = -yr^2$.

These boundary conditions are believed to be superior to specifying either potential flow or uniform velocity since eddies or vortices can pass through the downstream boundary. Also, because the velocity far away is not defined, the circulation there can change with time. Therefore, equation (11) correctly represents the vorticity transport through the downstream boundary. In equation (13), the absence of the tangential pressure derivative will not significantly affect the motion of a vortex through the boundary.

The surface pressure distribution is obtained by integrating the tangential component of the Navier-Stokes equation. That is,

$$p = \frac{L}{R}\frac{d\rho}{dr}\int_{o}^{\theta}\frac{\partial\omega}{\partial\rho}\,d\bar{\theta} \tag{14}$$

where $p(0) = 0$. The pressure coefficient C_p is, therefore, equal to $2p$. On the surface, the tangential stress is given by $\sigma_{12} = (L/R)\omega$. Both p and σ_{12} are made dimensionless with ρU^2. The coefficients of lift and moment are zero for symmetric geometries and flow fields; however, the coefficients of drag are computed as

$$C_D = \frac{drag}{(1/2)\rho U^2 l} = C_{DP} + C_{DF} \tag{15}$$

where

$$C_{DP} = \frac{4}{L}\int_{\pi}^{2\pi} p\,\frac{\partial y}{\partial\theta}\,d\theta \tag{16}$$

and

$$C_{DF} = -\frac{4}{R}\int_{\pi}^{2\pi}\omega\,\frac{\partial x}{\partial\theta}\,d\theta \tag{17}$$

where the subscripts P and F, respectively, represent the contributions due to pressure and viscous forces.

Equations (1) through (4) represent a nonlinear coupled set of partial differential equations. To reduce the difficulty in solving these equations, the nonlinearity may be removed by applying the Newton-Kantorovich transformation to the equations[9] or by performing a Taylor series expansion in function space to the nonlinear terms. Employing such a procedure alters the convection terms in the vorticity transport equation, and the linear approximation to this equation becomes

$$\begin{aligned} H^2 r^2 \frac{R}{L}\frac{\partial\omega}{\partial t} = {} & \left(\frac{d\rho}{dr}\right)^2 r^2\frac{\partial^2\omega}{\partial\rho^2} + \left(\frac{d\rho}{dr}\,r + \frac{d^2\rho}{dr^2}\,r^2\right)\frac{\partial\omega}{\partial\rho} + \frac{\partial^2\omega}{\partial\theta^2} \\ & - r\,\frac{d\rho}{dr}\,\frac{R}{L}\left[J\left(\frac{\omega_o,\Psi}{\rho,\theta}\right) + J\left(\frac{\omega,\Psi_o}{\rho,\theta}\right) - J\left(\frac{\omega_o,\Psi}{\rho,\theta}\right)\right] \\ & + O[\Delta\omega\Delta\Psi] \end{aligned} \tag{18}$$

where

$$\Delta\omega = \omega - \omega_o \tag{19}$$

and

$$\Delta\Psi = \Psi - \Psi_o$$

The functions ω_o and Ψ_o are initial guesses to the solutions ω and Ψ. These initial guesses must be sufficiently accurate such that the truncation error associated with approximating the nonlinear terms is no worse than the truncation error of the overall numerical technique.

NUMERICAL FORMULATION

The Navier-Stokes equations were solved by a three-point backward time differencing and implicit-explicit factored central space differencing scheme. The spatially factored, time-differenced expression for the linearized approximation to the vorticity transport equation[9] is

$$\left[1 - \frac{2\Delta t}{TA}\,\delta_\theta(\Psi_o)\right]\left[1 - \frac{2\Delta t}{TA}\,\delta_\rho(\Psi_o)\right]\omega^n = \frac{2\Delta t}{TA}\left[Q(\omega^n,\Psi_o) + F(\omega_o,\Psi_o,\Psi^n) + G(\omega_o,\Psi_o,\Psi^n)\right]$$

$$- \frac{1}{T}\left(T_1\omega^{n-1} + T_2\omega^{n-2}\right)$$

$$+ \frac{4(\Delta t)^2}{T^2}\,\frac{\delta_\theta(\Psi_o)}{A}\,\frac{\delta_\rho(\Psi_o)}{A}\,\omega^n$$

$$+ O(\Delta\omega\Delta\Psi\Delta t) + O(\Delta t)^3 \tag{20}$$

where the operators $\delta_\theta(\Psi_o)$ and $\delta_\rho(\Psi_o)$ are given as

$$\delta_\theta(\Psi_o) = \frac{\partial^2}{\partial\theta^2} + \frac{r}{3}\,\frac{d\rho}{dr}\,\frac{R}{L}\left[\frac{\partial}{\partial\theta}\left(\frac{\partial\Psi_o}{\partial\rho}\right) + \frac{\partial\Psi_o}{\partial\rho}\,\frac{\partial}{\partial\theta}\right] \tag{21}$$

$$\delta_\rho(\Psi_o) = \left(\frac{d\rho}{dr}\right)^2 r^2\,\frac{\partial^2}{\partial\rho^2} + \left(\frac{d\rho}{dr}\,r + \frac{d^2\rho}{dr^2}\,r^2\right)\frac{\partial}{\partial\rho} - \frac{r}{3}\,\frac{d\rho}{dr}\,\frac{R}{L}\left[\frac{\partial}{\partial\rho}\left(\frac{\partial\Psi_o}{\partial\theta}\right) + \frac{\partial\Psi_o}{\partial\theta}\,\frac{\partial}{\partial\rho}\right] \tag{22}$$

and the cross-derivative terms $Q(\omega^n,\Psi_o)$, $F(\omega_o,\Psi_o,\Psi^n)$, and $G(\omega_o,\Psi_o,\Psi^n)$ are given as

$$Q(\omega^n,\Psi_o) = -\frac{r}{3}\,\frac{d\rho}{dr}\,\frac{R}{L}\left[\frac{\partial}{\partial\theta}\left(\Psi_o\,\frac{\partial\omega^n}{\partial\rho}\right) - \frac{\partial}{\partial\rho}\left(\Psi_o\,\frac{\partial\omega^n}{\partial\theta}\right)\right] \tag{23}$$

$$F(\omega_o,\Psi_o,\Psi^n) = -\frac{r}{3}\frac{d\rho}{dr}\frac{R}{L}\left[\frac{\partial}{\partial\rho}\left(\frac{\partial\Psi^n}{\partial\theta}\omega_o - \frac{\partial\Psi_o}{\partial\theta}\omega_o\right) + \frac{\partial\Psi^n}{\partial\theta}\frac{\partial\omega_o}{\partial\rho}\right.$$

$$\left. - \frac{\partial\Psi_o}{\partial\theta}\frac{\partial\omega_o}{\partial\rho} + \frac{\partial}{\partial\theta}\left(\Psi^n\frac{\partial\omega_o}{\partial\rho} - \Psi_o\frac{\partial\omega_o}{\partial\rho}\right)\right] \tag{24}$$

$$G(\omega_o,\Psi_o,\Psi^n) = \frac{r}{3}\frac{d\rho}{dr}\frac{R}{L}\left[\frac{\partial}{\partial\theta}\left(\frac{\partial\Psi^n}{\partial\rho}\omega_o - \frac{\partial\Psi_o}{\partial\rho}\omega_o\right) + \frac{\partial\Psi^n}{\partial\rho}\frac{\partial\omega_o}{\partial\theta} - \frac{\partial\Psi_o}{\partial\rho}\frac{\partial\omega_o}{\partial\theta}\right.$$

$$\left. + \frac{\partial}{\partial\rho}\left(\Psi^n\frac{\partial\omega_o}{\partial\theta} - \Psi_o\frac{\partial\omega_o}{\partial\theta}\right)\right] \tag{25}$$

The values of the three-point backward time difference parameters are $T = 3$, $T_1 = -4$, and $T_2 = 1$. The transformation parameter A is

$$A = H^2r^2\frac{R}{L}$$

Let the initial guesses at the solution ω_o and Ψ_o be given by

$$\omega_o = 2\omega^{n-1} - \omega^{n-2} = \omega^n + O(\Delta t)^2 \tag{26}$$

$$\Psi_o = 2\Psi^{n-1} - \Psi^{n-2} = \Psi^n + O(\Delta t)^2 \tag{27}$$

except at the first two time steps where they are given as

$$\omega_o = \omega^{n-1} = \omega^n + O(\Delta t) \tag{28}$$

$$\Psi_o = \Psi^{n-1} = \Psi^n + O(\Delta t) \tag{29}$$

Hence,

$$\Delta\omega\Delta\Psi = O(\Delta t)^4 \tag{30}$$

$$F(\omega_o,\Psi_o,\Psi^n) = O(\Delta t)^2 \tag{31}$$

$$G(\omega_o,\Psi_o,\Psi^n) = O(\Delta t)^2 \tag{32}$$

except at the first two time steps. Therefore, except at the first two time steps, the terms F and G may be neglected because they are the same order as the overall truncation error. In addition, the second-order term on the right-hand side of equation (20) is made explicit by approximating it by

$$4\frac{(\Delta t)^2}{T^2}\frac{\delta_\theta(\Psi_o)}{A}\frac{\delta_\rho(\Psi_o)}{A}\omega^n = 4\frac{(\Delta t)^2}{T^2}\frac{\delta_\theta(\Psi_o)}{A}\frac{\delta_\rho(\Psi_o)}{A}\omega^{n-1} + O(\Delta t)^3 \tag{33}$$

The final second-order accurate time-differenced expression for the vorticity transport equation is then

$$\left(1 - \frac{2\Delta t}{TA}\,\delta_\theta(\Psi_o)\right)\left(1 - \frac{2\Delta t}{TA}\,\delta_\rho(\Psi_o)\right)\omega^n = \frac{2\Delta t}{TA}\,Q(\omega^n,\Psi_o) - \frac{1}{T}\left(T_1\omega^{n-1} + T_2\omega^{n-2}\right) + \frac{4(\Delta t)^2}{T^2}\,\frac{\delta_\theta(\Psi_o)}{A}\,\frac{\delta_\rho(\Psi_o)}{A}\,\omega^{n-1} + O(\Delta t)^3 \tag{34}$$

Consistent with the spatial factoring concept, equation (34) is split into two equations whose finite difference analogies each produce tridiagonal systems of equations. That is,

$$\left(1 - \frac{2\Delta t}{TA}\,\delta_\theta(\Psi_o)\right)\omega^* = \frac{2\Delta t}{TA}\,Q(\omega^n,\Psi_o) - \frac{1}{T}\left(T_1\omega^{n-1} + T_2\omega^{n-2}\right) + \frac{4(\Delta t)^2}{T^2}\,\frac{\delta_\theta(\Psi_o)}{A}\,\frac{\delta_\rho(\Psi_o)}{A}\,\omega^{n-1} + O(\Delta t)^3 \tag{35}$$

$$\left(1 - \frac{2\Delta t}{TA}\,\delta_\rho(\Psi_o)\right)\omega^n = \omega^* \tag{36}$$

The spatial derivatives associated with equations (35) and (36), as well as equation (19), were approximated by central differencing formulas everywhere except at the boundaries of the flow field. The truncation error for the vorticity transport equation is $O[(\Delta\rho)^2 + (\Delta\theta)^2 + (\Delta t)^2]$, except at the first two time steps where the temporal error is $O(\Delta t)$, because a two-point backward difference formula is required such that $T = 2$, $T_1 = -2$, and $T_2 = 0$.

The disturbance stream function equation is solved by the method of reference 12. The details of the procedure are not described here, but the truncation error of the disturbance stream function equation is $O[(\Delta\rho)^2 + (\Delta\theta)^2]$.

At the outer boundary, the finite difference forms of equations (35) and (36) are used to describe the vorticity condition, except that the diffusion terms are deleted and forward space differencing is used in the ρ direction. This formulation results in a first-order truncation error in the space variable ρ. The disturbance stream function at this boundary is obtained from the finite-difference form of equations (12) and (13):

$$\psi^n_{i,1} = \frac{1}{3}\left[\frac{2\Delta\rho}{\left(\frac{d\rho}{dr}\right)_1}\left(Hu_2{}^n + \frac{\partial y}{\partial r}\right)_{i,1} + 4\psi^n_{i,2} - \psi^n_{i,3}\right] \tag{37}$$

where

$$(u_2)^n_{i,1} = \frac{1}{T}\left[-2\Delta t\left[\left(u_1{}^n\omega^n\right)_{i,1} + \frac{(u_1{}^2 + U_2{}^2)^n_{i+1,1} - (u_1{}^2 + u_2{}^2)^n_{i-1,1}}{4\Delta\theta(rH)_{i,1}}\right] - \left(T_1u_2^{n-1} + T_2u_2^{n-2}\right)_{i,1}\right] \tag{38}$$

Along the lines of symmetry the boundary conditions $\omega = 0$ and $\psi = 0$ are specified. The no-slip boundary condition represented by equations (9) and (10) is satisfied by specifying the condition $\psi = 0$ along the boundary and by iteratively determining the surface vorticity that numerically enforces $\partial\psi/\partial\rho = 0$. The latter condition is accomplished by employing the method of Israeli.[11] That is, the surface vorticity at a particular iteration "k" is related to $\partial\psi/\partial\rho$ and the surface vorticity at the previous iteration "k-1" by

$$\omega^k_{JL} = g\left.\frac{\partial\psi}{\partial\rho}\right|^{k-1}_{JL} + \omega^{k-1}_{JL} \tag{39}$$

The coefficient g is a relaxation parameter whose optimum value is determined in reference 11 for boundary-layer type flows. For the fine grids and relatively large time steps used in the present study, the equations defining the optimum value of g as given in reference 11 may be approximated to the first order in $\frac{\Delta r_{JL}}{\sqrt{\nu\Delta t}}$ as

$$g \sim \sqrt{\frac{R}{\Delta t}} \tag{40}$$

where Δr_{JL} is the normal distance from the surface to the next grid point and ν, R, and Δt are the kinematic viscosity, Reynolds number, and time step size, respectively. The value of g for a given geometry and computational mesh must be determined manually once for a particular Reynolds number and time step size. Then, to determine the value of g at any other Reynolds number or time step size, equation (40) may be used with reasonable accuracy. In fact, figure 2 is a log-log plot of g versus Δt for a NACA 0012 airfoil at a Reynolds number of 10^4 using a 65 × 84 computational mesh. Equation (40) is represented in the figure by the straight line and optimum values of g determined manually are shown by the symbols. Note that the agreement is reasonable. In fact, the same calculations using the manually determined g required only a few percent less compute time than the value of g determined by equation (40). Furthermore, the savings in engineering and compute time by not manually searching for the optimum value of g more than makes up for the difference. More accurate formulations of the optimum value of g could be determined. However, for the purposes of the current study, this did not appear to be warranted.

In solving the systems of equations described by equations (2), (35), and (36), together with the boundary conditions (37), (38), and (39), a mixed iterative/noniterative procedure is used. Iteration is required because ω^n is contained in the term $Q(\omega^n,\Psi_o)$ on the right-hand side of equation (35). Hence, equations (2), (35), and (36) must be solved at each time step by iterative improvement. In addition, the boundary conditions (37), (38), and (39) are iterative in nature, hence they must also be satisfied by iterative improvement at each time step. However, the coefficient matrices of equations (35) and (36) do not need to be iteratively improved at each time step. A considerable amount of compute time, therefore, is saved at each time step by calculating these matrices and performing the forward elimination upon them outside the iteration loop. Then, in iteratively improving the values of ω^n in $Q(\omega^n,\Psi_o)$ and solving for ω^* and a new ω^n, only back substitutions need be performed. Convergence of the above-described iteration procedure was considered achieved when the change in surface vorticity between successive iterations was less than a prescribed value, typically 10^{-3} or 10^{-4}.

Computations of pressure coefficients on the surface and a determination of the loads are made at each time step with a finite-difference integration formula derived by combining two four-point expressions (in order to have a lower effective truncation error). The details of the formula may be found in reference 13.

DISCUSSION OF RESULTS

The present numerical technique was used to perform flow-field calculations for four test cases. These test cases included a steady-state solution for a circular cylinder at Reynolds number 15, a steady-state solution for an NACA 0012 airfoil at zero angle of attack at a Reynolds number of 10^3, and a steady-state solution and a time-accurate solution for the same airfoil at a Reynolds number of 10^4. Results were also obtained for the same airfoil at a Reynolds number of 10^5. The results for that test case, however, indicated that the flow field in the separation zone was unsteady at this Reynolds number. At this time it is not known whether this unsteadiness is due to numerical problems or whether it is a true flow-field phenomena; therefore, the results at this Reynolds number are not presented here.

A summary of the results of all test cases is presented in table 1. Included in the table are the compute times required for a steady-state solution on a CDC 7600 computer as well as the number and size of the time steps used and the size of the computational grid. All test cases were initiated from an impulsive start and computed to a steady-state solution. A detailed discussion of the results of each test case is given below.

Circular Cylinder at Re = 15

The circular cylinder test case was performed on a 33 × 40 grid in the half-plane. Plots of the steady-state surface vorticity and pressure

coefficient distributions are shown in figure 3. Comparisons of the results are made with Mehta's[9] numerical technique. As seen in the figure the results are in excellent agreement. Since only a steady-state solution was desired for this test case, no attempt was made to obtain time accuracy. As seen in table 1 the total compute time required to obtain the solution was 2.5 sec. A total of eight time steps were taken and the time step sizes (non-dimensionalized as $U\Delta t/l$) were 2.5 diam each. The cylinder traveled a distance of 20 diam during this time. The number of iterations required to obtain a converged solution at each time step varied from 21 at the first time step to 7 at the last time step.

NACA 0012 Airfoil at $Re = 10^3$

A computational grid in the half-plane of 65 × 48 was used to determine the flow field about the NACA 0012 airfoil at a Reynolds number of 10^3. Plots of the steady-state surface vorticity and pressure coefficient distributions are shown in figure 4. As shown in table 1, a total compute time of 24.8 sec was required to obtain this solution. The size of the time steps was initially 0.269 chord. However, the time step size was doubled after 10 time steps. A total of 23 time steps was used to obtain the steady-state solution, and the airfoil traveled a distance of 9.69 chords during this time. The number of iterations required for convergence at each time step varied from a maximum of 32 at the first time step to a minimum of 8 at the last time step.

NACA 0012 Airfoil at $Re = 10^4$

Two test cases were performed using a 65 × 84 computational mesh for the NACA 0012 airfoil at a Reynolds number of 10^4. The results of both test cases are shown in figure 5 as plots of the surface vorticity and pressure coefficient distributions. The results of both test cases are also compared with computations using Mehta's[9] numerical technique.

The first test case was performed to determine the steady-state solution only. This test case required 49.7 sec of compute time. Since time accuracy was not a consideration, the initial time step size was set at 0.138 chord, then doubled every 10 time steps. The steady-state solution was obtained after the airfoil had traveled about 9.67 chords, hence a total of 30 time steps was needed in obtaining the results. The number of iterations required for convergence at each time step varied from 32 at the first couple of time steps to 10 at the final time step.

The second test case at this Reynolds number was performed in order to obtain a time-accurate solution until a steady state was achieved. Therefore, the calculation was initiated with a smaller time step, 0.00276 chord. However, as before, the time step size was doubled every ten time steps until the airfoil had traveled about 9.88 chord lengths. The total number of time steps required to obtain this solution was 84, while the total compute time required was only 88 sec. The number of iterations required for convergence

of the surface vorticity varied from a maximum of 23 to a minimum of 6. The maximum occurred at the first time step and the minimum occurred at the tenth time step. Each time the time step was doubled, the number of iterations increased then gradually decreased from time step to time step until the time step doubled again. In general, fewer iterations were required for convergence for smaller time steps than for larger ones.

As seen in figure 5, both test cases were in excellent agreement with each other as well as with the solutions obtained using Mehta's[9] numerical technique.

CONCLUSIONS

Based on the results obtained to date, the present method appears capable of obtaining rapid steady-state and time-accurate solutions to the incompressible time-dependent Navier-Stokes equations. It has been successfully applied to a circular cylinder at a Reynolds number of 15 and an NACA 0012 airfoil at Reynolds numbers of up to 10^4 using fine computational grids. The numerical technique itself may be extended to representations of the Navier-Stokes equations in the primitive variables u, v, and p and therefore to three-dimensional flows. It may also be extended to the time-averaged Navier-Stokes equations with turbulence modeling.

ACKNOWLEDGMENT

The author would like to express gratitude to Dr. Ralph E. Gabrielsen of Ames Research Center and Dr. Unmeel B. Mehta of Stanford University. Dr. Gabrielsen originated the idea of applying the Newton-Kantorovich concept to the time-dependent Navier-Stokes equations, and it was through his scientific curiosity and impetus that this investigation was brought about. In addition, his guidance regarding the mathematical foundations of linearizing the Navier-Stokes equations was invaluable. Dr. Mehta graciously allowed us to use his excellent computer code during the course of this investigation. The numerical technique reported in this paper is an outgrowth of his numerical technique, and much of the improvement in the technique for our applications was due to his valuable suggestions.

REFERENCES

1. MacCormack, R. W.: An Efficient Numerical Method for Solving the Time-Dependent Compressible Navier-Stokes Equations at High Reynolds Number. NASA TM X-73,129, 1976.

2. Beam, R. M.; and Warming, R. F.: An Implicit Factored Scheme for the Compressible Navier-Stokes Equations. AIAA Paper 77-645, Albuquerque, New Mexico, June 1977.

3. Roache, P. J.: A Semidirect Method for Internal Flows in Flush Inlets. AIAA Paper 77-647, Albuquerque, New Mexico, June 1977.

4. Reddy, R. N.; and Thompson, J. F.: Numerical Solution of Incompressible Navier-Stokes Equations in the Integro-Differential Formulation Using Boundary-Fitted Coordinate Systems. AIAA Paper 77-650, Albuquerque, New Mexico, June 1977.

5. Wu, J. C.; and Sampath, S.: A Numerical Study of Viscous Flow Around an Airfoil. AIAA Paper 76-337, San Diego, California, July 1976.

6. Thames, F. C.: Numerical Solution of the Incompressible Navier-Stokes Equations About Arbitrary Two-Dimensional Bodies. Ph.D. Dissertation, Mississippi State University, 1975.

7. Ghia, K. N.; Hankey, W. L.; and Hodge, J. K.: Study of Incompressible Navier-Stokes Equations in Primitive Variables Using Implicit Numerical Technique. AIAA Paper 77-648, Albuquerque, New Mexico, June 1977.

8. Gabrielsen, R. E.: An Effective Solution to the Nonlinear, Nonstationary Navier-Stokes Equations for Two Dimensions. NASA TM X-62,493, 1975.

9. Davis, J. E.; Gabrielsen, R. E.; and Mehta, U. B.: A Solution to the Navier-Stokes Equations Based Upon the Newton-Kantorovich Method. NASA TM-78,437, 1977.

10. Mehta, U. B.: Dynamic Stall of an Oscillating Airfoil. AGARD Paper No. 23, Ottawa, Canada, 1977.

11. Israeli, M.: On the Evaluation of Iteration Parameters for Boundary Vorticity. Studies in Applied Mathematics, vol. 51, no. 1, March 1972.

12. Buzbee, B. L.; Golub, G. H.; and Nielson, C. W.: On Direct Methods for Solving Poisson's Equation. SIAM Journal of Numerical Analysis, vol. 7, 1970, pp. 627-656.

13. Mehta, U. B.; and Lavan, Z.: Starting Vortex, Separation Bubbles, and Stall — A Numerical Study of Laminar Unsteady Flow Around an Airfoil. J. of Fluid Mech., vol. 67, 1975, pp. 227-256.

FIGURE CAPTIONS

Figure 1.- Domain of calculation, boundary conditions, and grid notation.

Figure 2.- Comparisons of the optimum value of g as determined manually and by equation 40.

Figure 3.- Surface vorticity and pressure coefficient distributions on a circular cylinder; Re = 15.

Figure 4.- Surface vorticity and pressure coefficient distributions on a 12% thick symmetrical airfoil; $\alpha = 0$; $Re = 10^3$.

Figure 5.- Surface vorticity and pressure coefficient distributions on a 12% thick symmetrical airfoil; $\alpha = 0$; $Re = 10^4$.

TABLE 1. SUMMARY OF COMPUTATION TIMES FOR VARIOUS TEST CASES USING PRESENT TECHNIQUE

TEST CASE	TOTAL COMPUTE TIME (CDC 7600), seconds	TOTAL TIME STEPS TO STEADY STATE	TIME STEP SIZES $\left(\frac{U\Delta t}{l}\right)$	GRID ($\theta \times r$)
CIRCULAR CYLINDER AT Re=15	2.5	8	2.5	(33 × 40)
NACA 0012 AIRFOIL AT Re=10^3	24.8	23	0.269 TO 0.539	(65 × 48)
NACA 0012 AIRFOIL AT Re=10^4	49.7	30	0.138 TO 0.553	(65 × 84)
	88.0	84	0.00276 TO 0.707	(65 × 84)

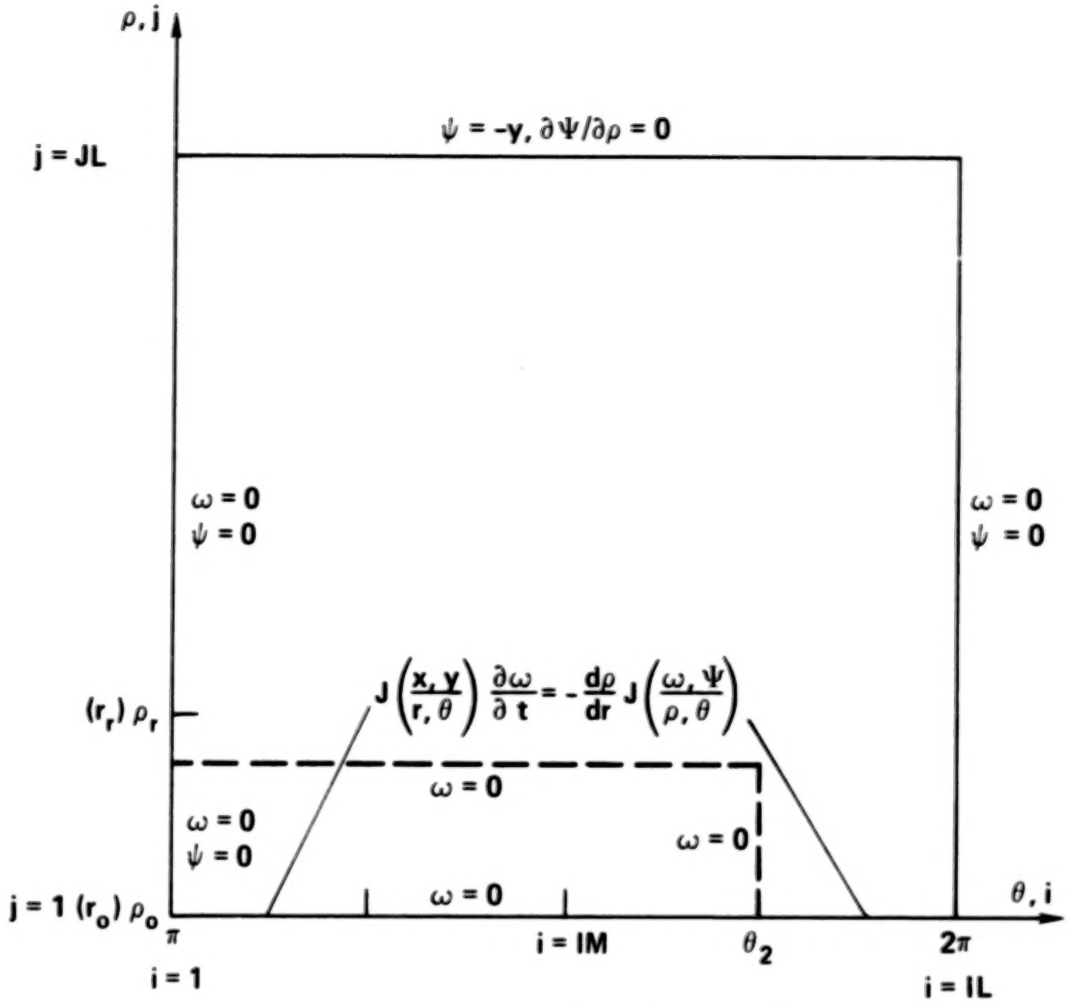

$$\frac{\partial U_2}{\partial t} = -\left[\frac{1}{2H} \partial \frac{(U_1^2 + U_2^2)}{\partial \theta} + U_1\, \omega\right]$$

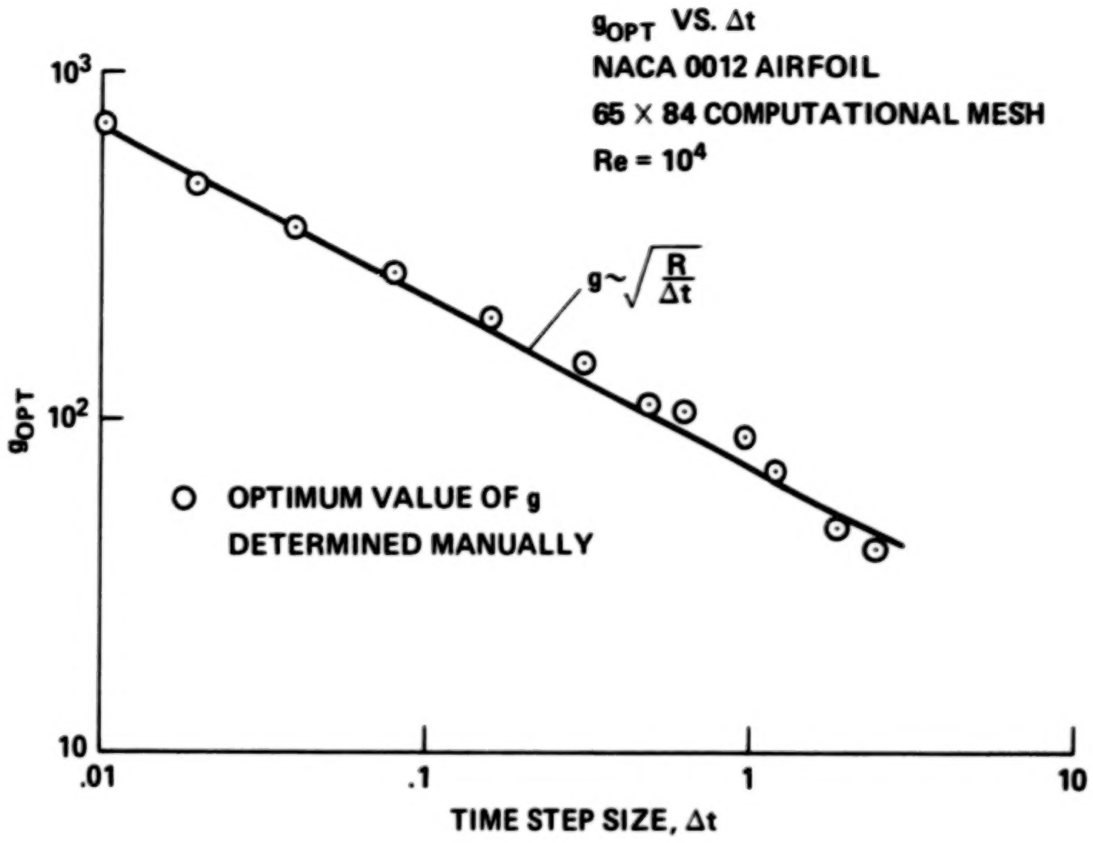
g_{OPT} VS. Δt
NACA 0012 AIRFOIL
65 X 84 COMPUTATIONAL MESH
Re = 10^4
$g \sim \sqrt{\frac{R}{\Delta t}}$
10^3
10^2
10
g_{OPT}
O OPTIMUM VALUE OF g
DETERMINED MANUALLY
.01
.1
1
10
TIME STEP SIZE, Δt

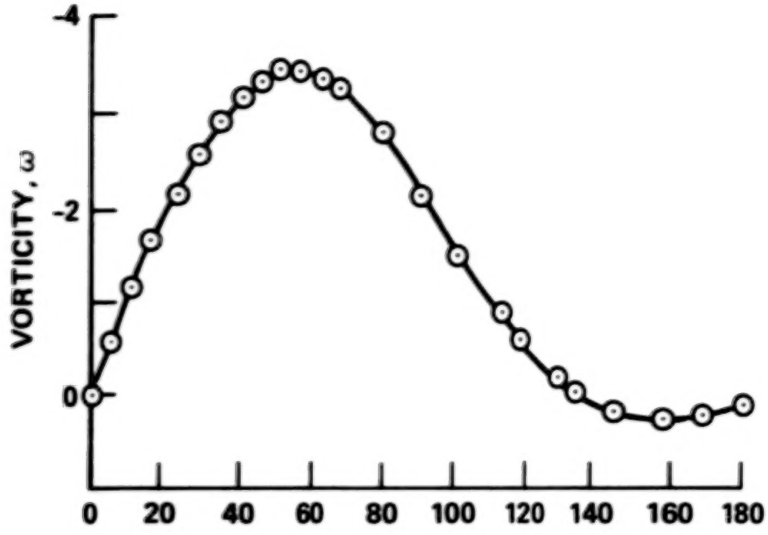
VORTICITY, ω
-4
-2
0
0 20 40 60 80 100 120 140 160 180

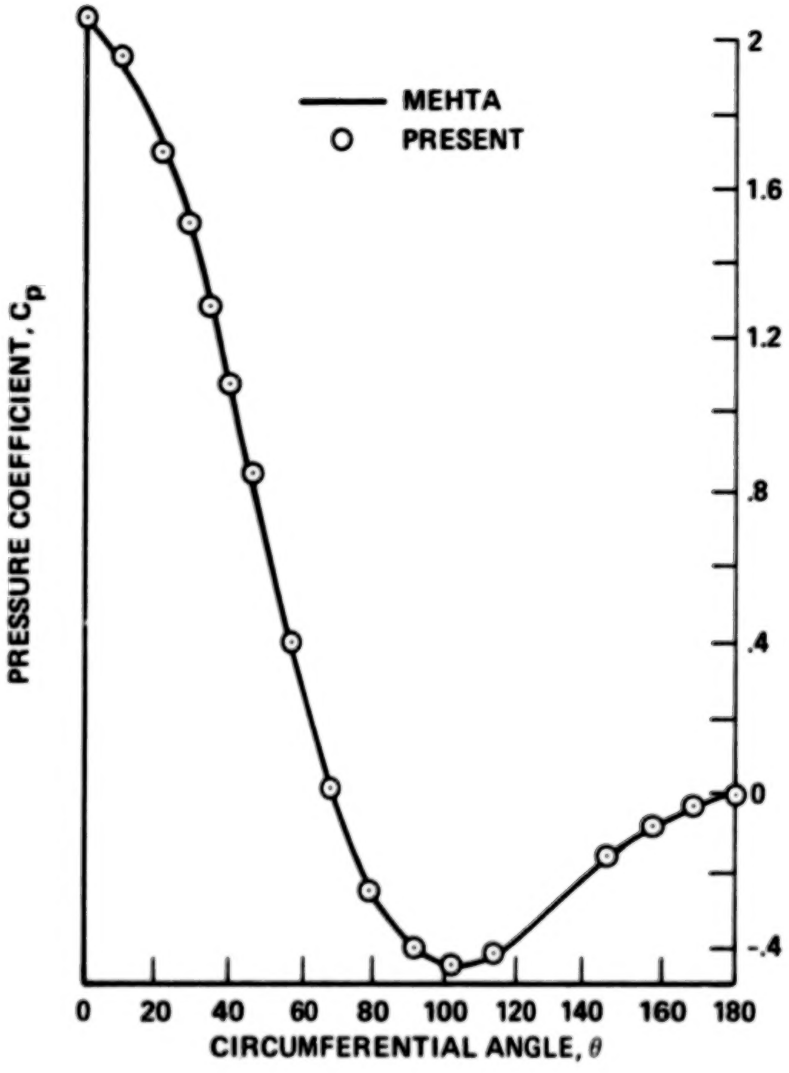
MEHTA
PRESENT
PRESSURE COEFFICIENT, C_p
2
1.6
1.2
.8
.4
0
-.4
0 20 40 60 80 100 120 140 160 180
CIRCUMFERENTIAL ANGLE, θ

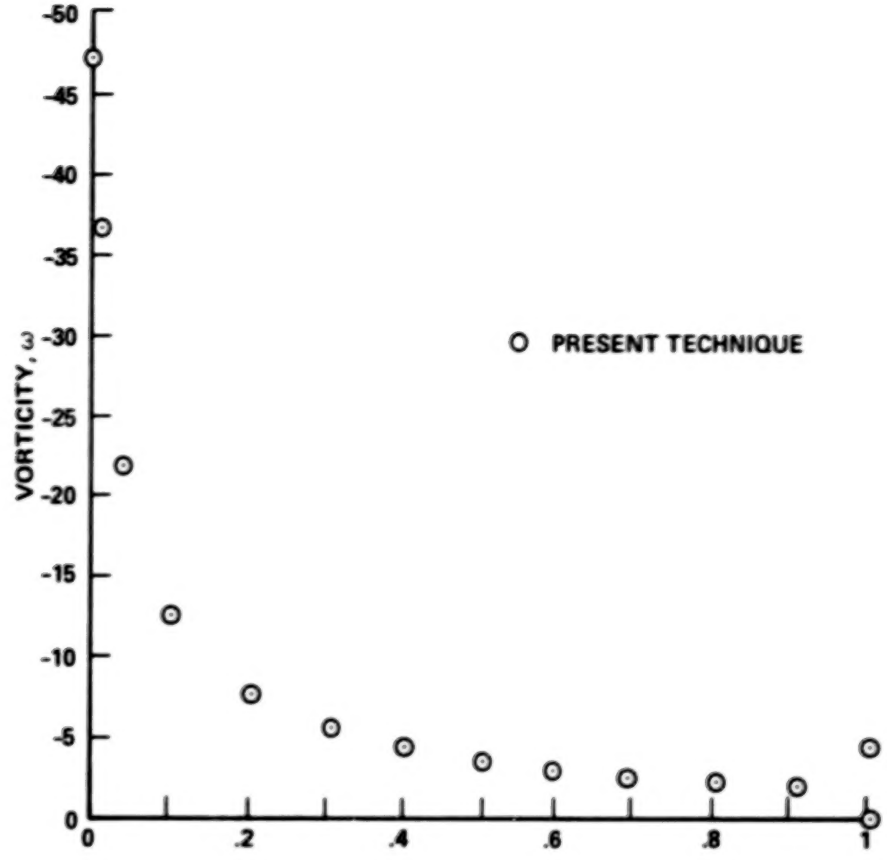
-50
-45
-40
-35
-30
-25
-20
-15
-10
-5
0
VORTICITY, ω
PRESENT TECHNIQUE
0
.2
.4
.6
.8
1

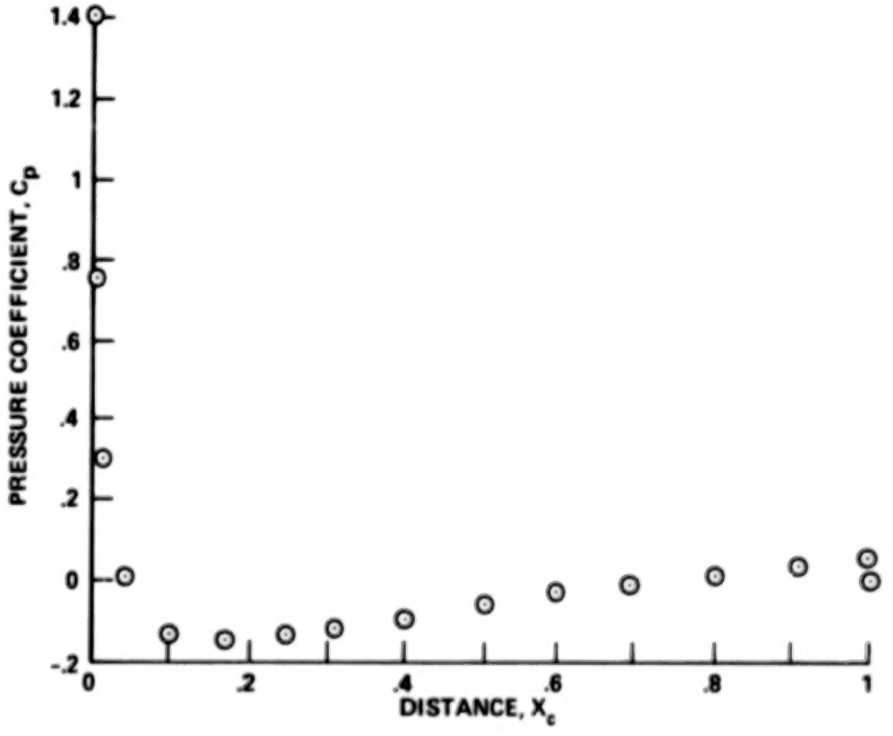
1.4
1.2
1
.8
.6
.4
.2
0
-.2
PRESSURE COEFFICIENT, C_p
0
.2
.4
.6
.8
1
DISTANCE, X_c

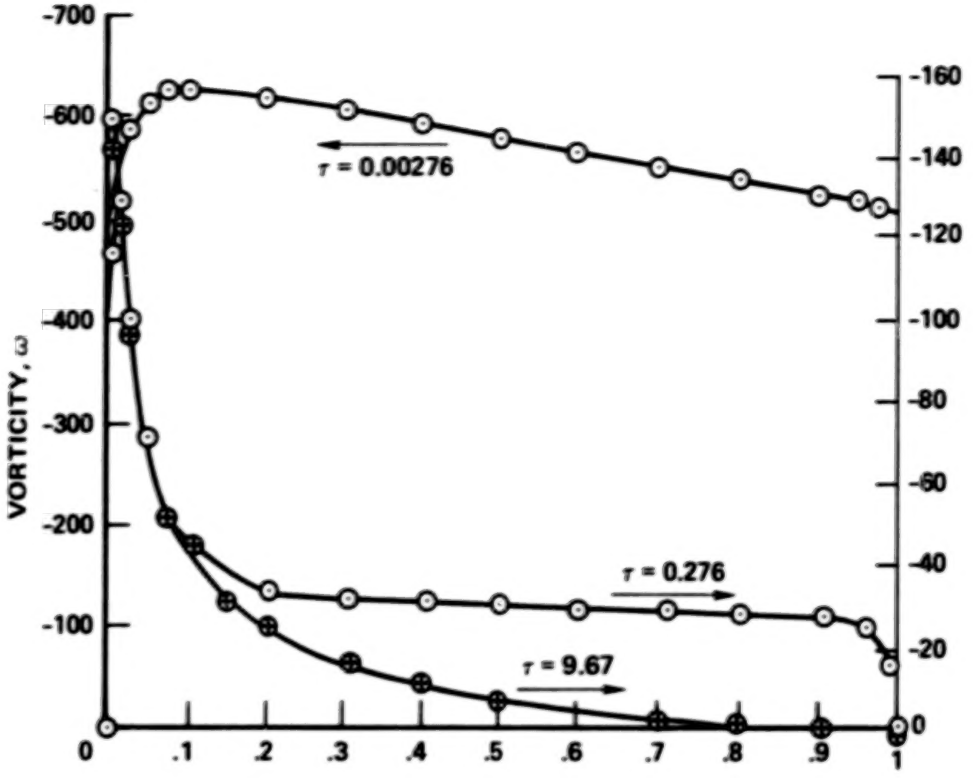
VORTICITY, ω
-700
-600
-500
-400
-300
-200
-100
0
-160
-140
-120
-100
-80
-60
-40
-20
0
τ = 0.00276
τ = 0.276
τ = 9.67
0
.1
.2
.3
.4
.5
.6
.7
.8
.9
1

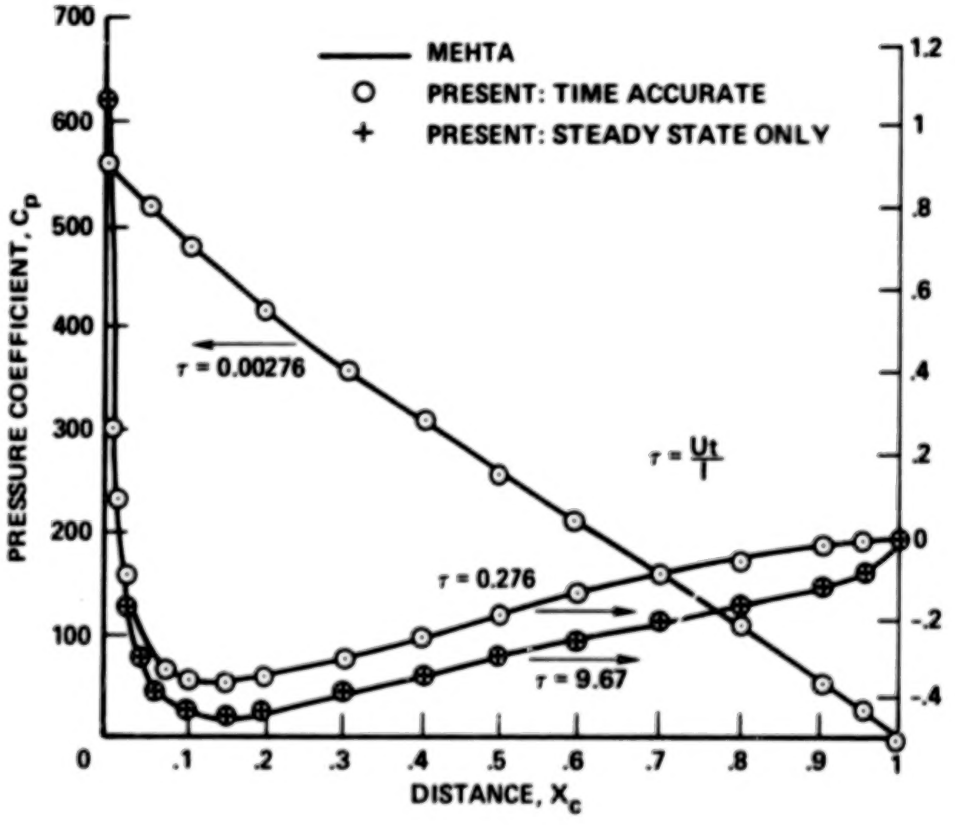
MEHTA
PRESENT: TIME ACCURATE
PRESENT: STEADY STATE ONLY
PRESSURE COEFFICIENT, C_p
700
600
500
400
300
200
100
0
1.2
1
.8
.6
.4
.2
0
-.2
-.4
τ = 0.00276
τ = 0.276
τ = 9.67
$\tau = \frac{Ut}{l}$
0
.1
.2
.3
.4
.5
.6
.7
.8
.9
1
DISTANCE, X_c

1. Report No.	2. Government Accession No.	3. Recipient's Catalog No.
NASA CR-3330		

4. Title and Subtitle "A Rapid Implicit-Explicit Solution to the Two-Dimensional Time-Dependent Incompressible Navier-Stokes Equations"	5. Report Date October 1980 6. Performing Organization Code
7. Author(s) Joseph E. Davis	8. Performing Organization Report No. 10. Work Unit No.
9. Performing Organization Name and Address Joseph E. Davis 20780 Sevilla Lane Saratoga, CA 95070	11. Contract or Grant No. A50807B 13. Type of Report and Period Covered Contractor Report
12. Sponsoring Agency Name and Address National Aeronautics and Space Administration Washington, D. C.	14. Sponsoring Agency Code

15. Supplementary Notes

Ames Technical Monitor: Warren Ahtye
Final Report

16. Abstract

A rapid implicit-explicit finite difference scheme has been developed for the numerical solution of the time-dependent, incompressible, two-dimensional Navier-Stokes equations in conservation-law form using vorticity and stream function variables. The algorithm is second-order time-accurate and spatially factored. The systems of equations are solved at each time step by an iterative technique. Numerical results have been obtained with the technique for a circular cylinder at a Reynolds number of 15, and an NACA 0012 airfoil at zero angle of attack at Reynolds numbers of 10^3 and 10^4. The results are in agreement with another numerical technique, and the computing time required to obtain the steady-state solution at the Reynolds number of 10^4 was 49.7 sec on a CDC 7600 computer using a 65 x 84 computational grid.

17. Key Words (Suggested by Author(s))	18. Distribution Statement
Airfoils, Transient Flow, Navier-Stokes, Laminar Flow, Finite Differences	Unclassified - Unlimited Star Category - 34

19. Security Classif. (of this report)	20. Security Classif. (of this page)	21. No. of Pages	22. Price*
Unclassified	Unclassified	21	A02

*For sale by the National Technical Information Service, Springfield, Virginia 22161

NASA-Langley, 1980

90 %

END

12-28-80